Measurements of Resonant Raman scattering Differential Cross sections for W using Synchrotron Radiation

Anil Kumar, M.K. Tiwari*, G.S. Lodha* and Sanjiv Puri

Department of Basic and Applied Sciences, Punjabi University, Patiala-147002, Punjab, India.
*-Synchrotron Utilization and Materials Research Division, RRCAT, Indore 452013, India.
Corresponding author's e-mail address: sanjivpurichd@yahoo.com

Abstract

The differential cross sections for the $(L_i\text{-}S_j)$ (i=1-3 and Sj=M_1, M_4, M_5, N_4) Raman Resonant scattering (RRS) peaks have been measured at different incident photon energies slightly less than (a few eV) the L_i(i=1-3) absorption edges of $_{74}$W. The present measurements were performed using the micro-focus X-ray fluorescence beam-line (BL-16) of INDUS-2 synchrotron radiation facility. The ratios $(L_3\text{-}M_1)/(L_3\text{-}M_{4,5})$ and $(L_2\text{-}N_4)/(L_2\text{-}M_4)$ evaluated from these presently measured differential cross sections are found to be higher than the calculated fluorescent x-ray intensity ratios, $I_{Ll}/I_{L\alpha}$ and $I_{L\gamma 1,5}/I_{L\beta}$, respectively by 10-25%.

1. Introduction

At incident photon energies in the vicinity of the L_i(i=1-3) sub-shell absorption edge-energies for a given element, the near-edge processes such as X-ray absorption fine structure (XAFS/EXAFS) [1] and the resonant Raman scattering (RRS) [2] becomes predominant. The RRS occurs at energies just below the absorption edge energies and the XAFS just above the absorption edge energies. At the incident photon energies slightly less than (a few eV) the shell / sub-shell binding energy, the RRS process proceeds by creation of a virtual hole in the respective shell / sub-shell (intermediate state) with the corresponding electron excited to an unoccupied state. This virtual hole is filled by some outer shell / sub-shell electron thereby resulting in emission of a photon having energy equal to the difference between the final and initial holes states. Different theoretical aspects of the RRS process are discussed elsewhere [3]. The experimental data on the L_i(i=1-3) sub-shell RRS cross sections are scarce [4]. The reported RRS cross sections were measured for a few medium Z elements only at single incident photon energy using quasi monochromatic photon beams. In the present work, the differential cross sections for the $(L_i\text{-}S_j)$ (*i*=1-3 and Sj=M_1, M_4, M_5, N_4) RRS peaks have been measured at different incident photon energies

slightly less than (a few eV) the L_i(i=1-3) absorption edges of $_{74}$W.

2. Experimental Details

The present measurements were performed using the micro-focus X-ray fluorescence beam-line (BL-16) of INDUS-2 synchrotron radiation facility. The salient features of BL-16 beam-line and details of the X-ray fluorescence (XRF) setup are given elsewhere [5]. The electron storage ring at INDUS-2 was operated at 2.53 GeV with a nominal current of 100 mA. A Si (111) double crystal monochromator (DCM) capable of tuning the photon energy in the range 4-15 keV with energy resolution $\sim 10^{-3}$-10^{-4} was used to obtain a monochromatic photon beam of desired energy on the sample position. The target holder was placed at 45° with respect to the incident beam direction.
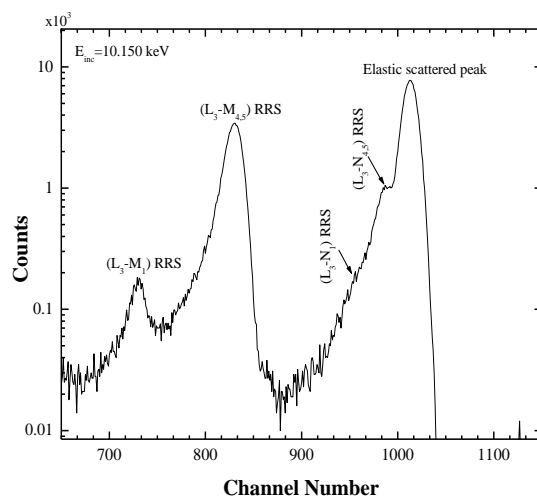

Figure 1: A typical spectrum of $_{74}$W target at 10.150 keV incident photon energy (64 eV below the L_3 edge energy) depicting the L_3 sub-shell RRS peaks.

The monochromatic beam was allowed to pass through an ionization chamber (aperture size: 10 mm×6 mm; FMB OXFORD, UK) before reaching the target in order to monitor the incident photon beam intensity (I_o). The X-ray detector was placed at 90° with respect to the incident beam direction. Spectroscopically, pure self-supporting $_{74}$W metallic foil of thickness 96 mg/cm^2 procured from Sigma-Aldrich was used as the target. The fluorescent/scattered X-rays emitted from the target were detected using a Vortex-EX90 silicon drift detector (50 mm^2×350 µm, FWHM~140 eV at 5.89 keV, Be window thickness~1 mil, SII Nano Tech. Inc., USA) coupled to a digital pulse processor (XIA LLC, USA). At 10.150 keV incident photon energy (64 eV below the L_3 edge) the observed (L_3-Sj) (Sj=M_1, $M_{4,5}$, N_1 and $N_{4,5}$) RRS peaks are shown along with the elastic scattered peak in Figure 1. It may be mentioned that the energies of different (L_i-S_j) RRS peaks have been determined as (E_{inc}-E_{Sj}), where E_{inc} represents the incident photon energy (below the L_i sub-shell absorption edge) and E_{Sj}, the binding energy of the sub-shell containing the final hole.

3. Evaluation Procedure

The (L_i-S_j) (i=2, 3 and Sj=M_1, M_4, M_5, N_4) RRS differential cross sections at different incident photon energies have been evaluated using the relation

$$\frac{d\sigma^{RRS}_{(Li-Sj)}}{d\Omega} = \frac{N_{(Li-Sj)}}{4\pi\, I_o G\varepsilon\beta^{RRS}_{(Li-Sj)}m}$$

where $N_{(Li-Sj)}$ represents the counts per unit time under the (Li-Sj) RRS peak, ε is the detector efficiency at (L_i-S_j) RRS peak energy, and $\beta^{RRS}_{(Li-Sj)}$ is the self-absorption correction factor which accounts

for the absorption of incident and scattered photons in the target and m is the mass (g/cm^2) of the target. The values of the self-absorption correction factor (β), the peak areas for different (L_i-S_j) RRS peaks observed at different incident photon energies and the product, Gε, have been evaluated as explained elsewhere [6].

4. Results

The present measured differential cross sections for the (L_i-S_j) (i=2, 3 and Sj=M_1, M_4, M_5, N_4) RRS at different incident photon energies are given in Table 1. The ratios (L_3-M_1)/(L_3-$M_{4,5}$) and (L_2-N_4)/(L_2-M_4) deduced from the presently measured differential RRS cross sections are found to be higher by 10-25% than the calculated fluorescent X-ray intensity ratios, $I_{Ll}/I_{L\alpha}$ and $I_{L\gamma1,5}/I_{L\beta}$ taken from reference [7].

References

[1] J. J. Rehr. Radiation Physics Chemistry 75 (2006) 1547 and references therein.

[2] S. Manninen. Radiation Physics Chemistry 50, (1997) 77.

[3] J. Tulkki J and T. Aberg. J. Phys. B. 15 (1982) L435.

[4] A. G. Karydas, S. Galanopoulos, Ch. Zarkadas, T. Paradellis and N Kallithrakas-Kontos. J. Phys.: Condens. Matter 14, (2002) 12367 and references therein.

[5] M.K. Tiwari, P. Gupta, A.K. Sinha, C.K. Garg, A.K. Singh, S.R. Kane, S.R. Garg and G.S. Lodha. J. Synchrotron Radiation 20 (2013) 386–389.

[6] Anil Kumar and Sanjiv Puri. Radiation Physics and Chemistry 81 (2012) 735.

[7] Sanjiv Puri. To appear in Atomic Data Nuclear Data Tables, (2013).

Table 1: Present measured (L_i-S_j) (i=2, 3 and Sj=M_1, M_4, M_5, N_4) RRS differential cross sections at different incident photon energies for tungsten. The present measured RRS cross section ratios are also compared with the corresponding theoretical intensity ratios of fluorescent X-rays for tungsten.

E (KeV)	ΔE (eV)	RRS cross sections (b/sr)				RRS Cross section ratio and theoretical fluorescent x-ray intensity ratios			
		(L_3-M_1)	(L_3-$M_{4,5}$)	(L_2-M_4)	(L_2-N_4)	(L_3-M_1)/(L_3-$M_{4,5}$)	$\frac{I_{Ll}}{I_{L\alpha}}$ (Thr)	(L_2-N_4)/(L_2-M_4)	$\frac{I_{L\gamma1,5}}{I_{L\beta}}$ (Thr)
10.150	E_{L3}-E_{inc} = 64	0.475±0.04	11.7±0.92	--	--	0.0408±0.003	0.0469	--	--
11.500	E_{L2}-E_{inc} = 51	--	--	8.59±0.60	2.24±0.21	--	--	0.261±0.002	0.206
11.520	E_{L2}-E_{inc} = 31	--	--	23.3±1.63	6.21±0.58	--	--	0.266±0.002	0.206
11.539	E_{L2}-E_{inc} = 12	--	--	93.2±6.52	20.9±1.99	--	--	0.225±0.002	0.206